

Confining layer influence on capacity of offshore caisson foundations

Le influence de la couche confinée sur la portance de les fondation *caisson en mer*

L.O. Mendes

Universidade de Brasilia, Brasília, Brazil

K.M. Briggs

University of Bath, Bath, United Kingdom

ABSTRACT: Regarding to offshore structures, such as jack-up platforms and wind turbines, one of the main concerns is about their foundations. In the British shore, for instance, the sand layer overlying the rock is not so deep, which can be an issue for the installation of shallow foundations. The traditional bearing capacity theory assumes an infinite depth of soil, but the presence of a hard layer underneath can affect the load. Then, this research project aimed to investigate the influence of this hard layer on the installation of offshore shallow foundations. To do so, loading tests were undertaken using a reduced scale model of a caisson foundation. This kind of foundation is positioned on the seabed and it is driven into the sand by the suction of the confined water. Then, the loading tests consisted on the penetration of the caisson model into 3 samples of sand using a press. The samples were placed inside a barrel, which was reinforced underneath with a birch plywood plate. An additional loading test was done, but without the plate. As a result, higher loads were observed with the decrease of the specimen heights, considering the same settlement of the caisson. In addition, higher loads were noticed for the tests with the plate compared with the test without the plate, and the difference between the loads for both cases increases with the settlement of the foundation. For future work, it is advisable to adapt the model in order to consider the suction effects.

RÉSUMÉ: En référence sur les structures en mer, comme les éoliennes, leur fondations sont une grande préoccupation. Dans la côte de la Grande-Bretagne, par exemple, la couche de sable qui recouvre la roche n'est pas très profonde, et ce fait peut influencer l'installation des fondations superficielles. Par contre, la théorie traditionnelle de la portance suppose que le sol a une profondeur infinie. Donc, ce projet a examiné l'influence de cette couche dure sur l'installation des fondations superficielles en mer, et une maquette de la fondation *caisson* a été utilisée. Cette type de fondation est positionnée dans le fond marin et est pénétrée dans le sable en raison de la succion de l'eau qui est confinée à l'intérieur de la fondation. Ensuite, pendant les tests, la maquette a été pénétrée dans 3 échantillons de sable, avec l'aide d'une presse. Les échantillons ont été mis dans un baril, et une contreplaqué de bouleau dur a été positionné sur le fond du baril. Un test supplémentaire a été fait sans le contreplaqué de bouleau. Le résultat, plus grandes charges ont été observées avec la diminution de la hauteur des échantillons pour la même déplacement du caisson. En outre, plus grandes charges ont été observées pour les tests avec le contreplaqué de bouleau en comparaison avec le test supplémentaire, sans le contreplaqué de bouleau, et la différence entre les charges pour les deux cas a augmenté avec le déplacement du caisson. Pour les projets futurs, l'adaptation de la maquette pour considérer les effets de la succion est recommandée.

Keywords: Offshore structures, caisson, confined layer, small scale tests

1 INTRODUCTION

1.1 Offshore caisson foundations

Offshore foundations are commonly used in structures like tidal turbines, offshore wind turbines and rigs. This kind of foundation must be designed considering the possible transference of the whole structure, as well as the cyclic loading due to the waves.

A very common kind of offshore foundation is the caisson. This foundation is commonly applied in offshore tidal and wind turbines, and consists in a skirt attached to a flat footing, creating a kind of a caisson on the seabed, as shown in Figure 1.

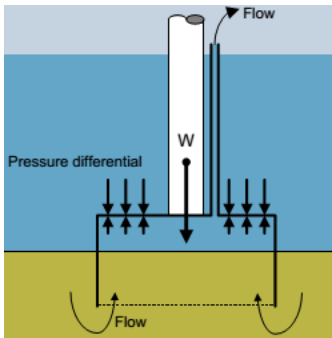


Figure 1. Caisson foundation (Byrne, 2011)

The installation of the caisson is described by Cotter (2009). The foundation is constructed onshore and it is placed on the seabed helped by a crane whilst some valves allow the air inside the foundation to escape. Once positioned, the caisson will penetrate the soil just with its self-weight. After this first displacement, the pump system starts to remove the water which is trapped inside the caisson, dropping the internal pressure. Consequently, the downward force caused by the water pushes the caisson a little further inside the soil. When the necessary penetration is reached, the pumps stop.

1.2 Confining Layer Influence on Capacity

The traditional theory of bearing capacity considers a soil layer with infinite thickness, even though the presence of a hard layer many meters

below the foundation can influence the amount of load that the soil can support. Then, consider the simplified bearing capacity equation by Terzaghi's theory (Cerato and Lutenegeger, 2006):

$$q_{ult} = 0.5\gamma BN_{\gamma} \quad (1)$$

In the Equation 1, q_{ult} is the ultimate capacity of footing, B is the footing width, γ is the soil unit weight and N_{γ} is the bearing capacity factor. If the layer between the footing and the hard layer is relatively thin, the bearing capacity factor N_{γ} should be modified to N_{γ}^* . Mandel and Salencon (1972, cited by Cerato and Lutenegeger, 2006) formulated a solution that established N_{γ}^* as a function of the effective friction angle (ϕ') and H/B ratio, where H is the thickness of the sand layer between the footing and the hard layer and B is the footing width; for the authors, the adoption of N_{γ}^* is necessary only if $H/B \leq 1$.

Cerato and Lutenegeger (2006) conducted a series of studies to investigate the influence of the rigid layer for $H/B > 1$. They also investigated the influence of the foundation shape on capacity, suggesting the following expression for the ultimate bearing capacity:

$$q_{ult} = 0.5\gamma BN_{\gamma}^*s_{\gamma}^* \quad (2)$$

In the Equation 2, s_{γ}^* is the modified shape factor. During their experiments, Cerato and Lutenegeger (2006) conducted tests using square and circular footings, which were loaded on a saturated sand layer. These tests were made using square and circular footings with widths varying between 0.102 m and 0.457 m. The target densities for sand were $Dr = 24\%$, 57% and 87% , and the H/B ratios were 0.5, 1, 2, 3 and 4.

As presented by Figure 2, it can be noticed that the values of N_{γ}^* start to converge at a H/B ratio between 3 and 4. Based on this, Cerato and Lutenegeger (2006) suggested the adoption of N_{γ}^* for $H/B \leq 3$. However, it is important to highlight that the values of N_{γ}^* were back calculated based

on empirical results for q_{ult} . Furthermore, the results also present a higher bearing capacity for square footings than for circular ones.

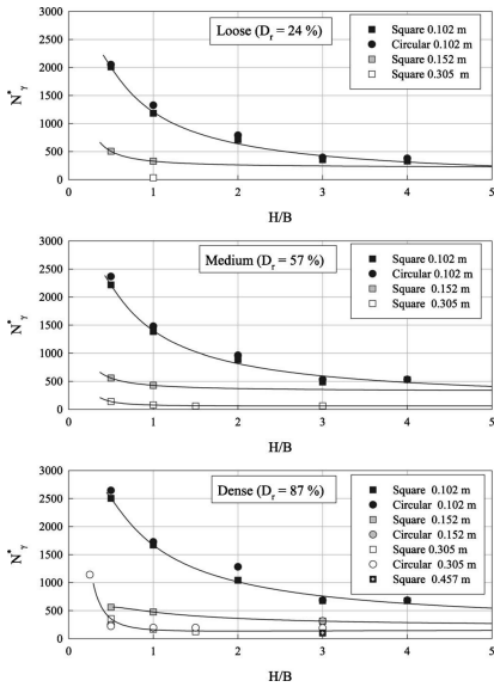


Figure 2. N_γ^* graphs for different footing widths (Cerato and Lutenegeger, 2006)

1.3 Aim and Objectives

This paper aims to measure the influence of a stiff confining layer on the bearing capacity of an offshore caisson foundation in sand. To do so, loading tests were done using a reduced scale model of a caisson foundation, which was settled into specimens of sand of different layer thickness, similarly to the tests conducted by Cerato and Lutenegeger (2006).

2 LABORATORY TESTS

This section will show the approaches to address the offshore foundations and the influence of a confined stiff layer on the capacity of an overlying sand layer. Three kinds of laboratory tests were conducted with samples of fine sand:

- Sieving test
- Triaxial compression test
- Footing (loading) test

The first two tests were chosen to give the parameters to prepare the third one, the footing loading test, which was the main focus of this project. In all of them, the sand was previously disaggregated as much as possible into small particles and the moisture contents of the samples were measured after the procedures.

2.1 Sieving test (BS 1377-2:1990)

The sieving test was conducted using 8 different sieves, with the following apertures: 8 mm, 4 mm, 2 mm, 1 mm, 500 μm , 250 μm , 125 μm and 63 μm . The sand was sieved by a vibrator plate, and the experiment was performed twice for an amount of 200 g of soil each time. As a result, an amount of 66% of the samples is fine sand ($0.06 \text{ mm} < \text{size} < 0.2 \text{ mm}$) and 33.7% is medium sand ($0.2 \text{ mm} < \text{size} < 0.6 \text{ mm}$). Figure 3 shows the particle size distribution graph.

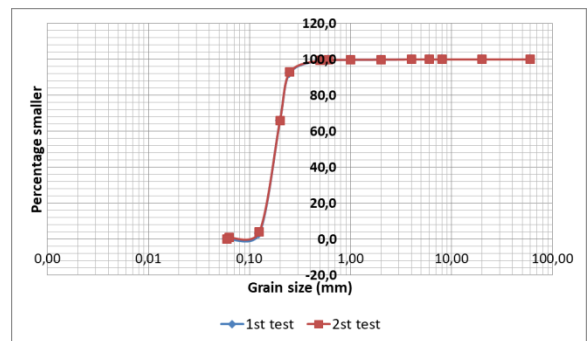


Figure 3. Particle size distribution

2.2 Triaxial compression test (BS 1377-8:1990)

The triaxial compression test was made in a drained condition (CD test); therefore, the strength parameters were calculated in terms of effective stresses. Table 1 shows the main parameters of the test, such as the cell pressure (P_c), porepressure (u) and the parameters of the

specimen (diameter - d, height - h, weight - w, and dry density - ρ_d).

Table 1. Triaxial test parameters

Pc (KPa)	u (KPa)	d (mm)	h (mm)	w (g)	ρ_d (kg/m ³)
300	250	70.8	130	725	1416.6
250	100	70.8	130	744	1453.7

Thus, Table 2 presents the results got from the triaxial test, such as the major and minor effective stresses (σ_1 and σ_3 , respectively), as well as the effective friction angle (ϕ') and the cohesion of the sand (c'), and Figure 4 illustrates the Mohr circles, in terms of effective stresses, as well as the failure envelope and its equation.

Table 2. Triaxial test results

Pc (KPa)	u (KPa)	σ_1 (KPa)	σ_3 (KPa)	ϕ'	c' (KPa)
300	250	223.1	50	37.2°	5.00
250	100	629.0	150		

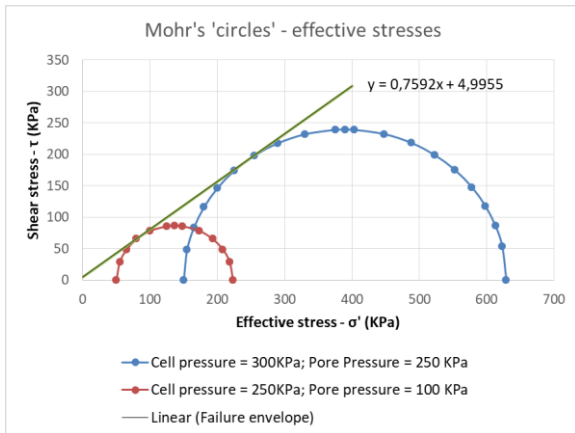


Figure 4. Mohr circles for the sand

2.3 Footing loading test

The loading tests were performed to address the capacity during the installation of a caisson foundation in sand, verifying the the influence of a stiff layer underneath. A model of a caisson foundation was fabricated in the laboratory with

steel, with a mass of 2218 g. Figure 5 exhibits a sketch of the footing with its dimensions and Figure 6 presents a picture of it.

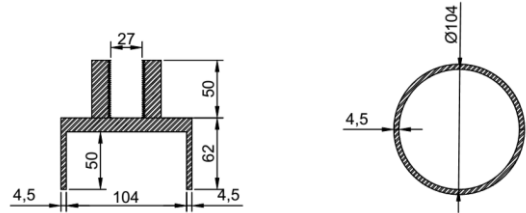


Figure 5. Sketch of the footing (dimensions in mm)



Figure 6. Photo of the footing

Also, specimens of sand were prepared, all with the same dry density target ($\rho_d = 1405 \text{ kg/m}^3$), based on the triaxial test results. The sand, which was previously wetted, was placed in a barrel 580 mm high, with a diameter of 580 mm. A tamper, with a mass of 4.72 kg, was also used to compact the sand. In addition, a timber plate made of birch plywood, with a diameter of 563 mm, 25 mm thick and with a mass of 4.28 kg, was placed beneath the barrel to reinforce its bottom, in order to simulate the confined stiff layer. According to BS EN 636:2003, plywood panels have high bending strength, with values varying between 5 N/mm² and 120 N/mm².

The specimens were built inside the barrel by a layering process. Each layer consisted on an amount of 18.56 Kg of dry sand poured into a height of 50 mm, considering the dry density target of 1405 kg/m³. For the purpose of this project, specimens with three different heights were prepared, Their heights were multiples of the mean diameter of the footing ($d_f = 109 \text{ mm}$),

which is not a multiple of 50. So, the height of the last layer was less than 50 mm and less sand had to be poured in this layer. Table 3 gives the parameters to build the specimens, such as the ratios between the height of the specimen and the diameter of the footing (H/d_f), the total weight of sand (W_s), the number of layers (n) and the amount of sand to be poured in the last layer (ΔW_s). Figure 7 also illustrates a sketch of the specimen for $H/d_f = 0.78$.

The footing was loaded into the specimen using a press, and the test was stopped when the tip of the footing reached 30 mm above the bottom of the barrel. Different rates of displacement were used throughout the tests for different intervals of settlements. Ultimately, the final heights of the specimens (H_f) were higher than those previously calculated due to an improper compaction, which resulted in densities slightly lower than 1405 kg/m^3 . Also, a complementary test was conducted using the same H/d_f for the first test ($H/d_f = 0.78$), but without the timber plate beneath the barrel, in order to compare the situations with and without the stiff layer underneath. So, Table 4 gives the final parameters for the tests (ρ_f : final dry density; M : moisture content; v : settlement velocity), Figure 8 displays the conduction of one of the loadings and Figures 9 to 12 show the graphs “load vs settlement” for each loading test.

Table 3. Estimated parameters for the samples

H/d_f	H (mm)	W_s (kg)	n	ΔW_s (kg)
0.78	85	31.55	2	13
1	109	40.46	3	3.34
2	218	80.92	5	6.68

Table 4. Final parameters of the samples

H/d_f	H (mm)	H_f (mm)	ρ_f (kg/m ³)	M (%)	v (mm/s)	
					Until 45 mm	After 45 mm
0.78	85	90	1326.82	15.99	0.01	0.05
1	109	124	1234.98	20.18	0.15	0.05
2	218	250	1225.10	15.15	0.15	0.05
0.78 (no timber plate)	85	93	1284.02	20.58	0.15	0,05

0.78	85	31.55	2	13
1	109	40.46	3	3.34
2	218	80.92	5	6.68

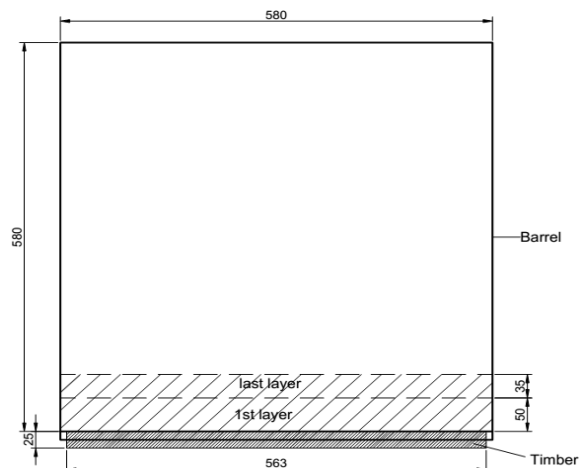


Figure 7. Sketch of the sample for $H/d_f = 0.78$ (dimensions in mm)

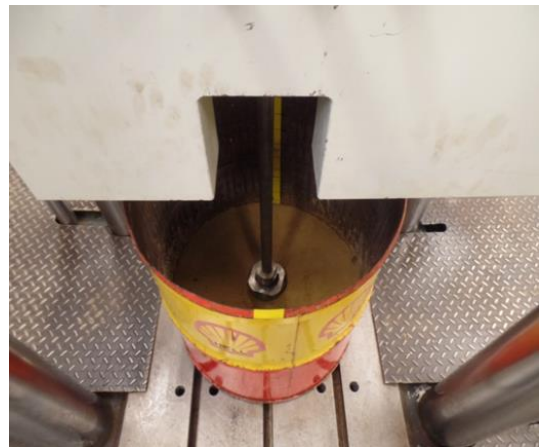


Figure 8. Loading test

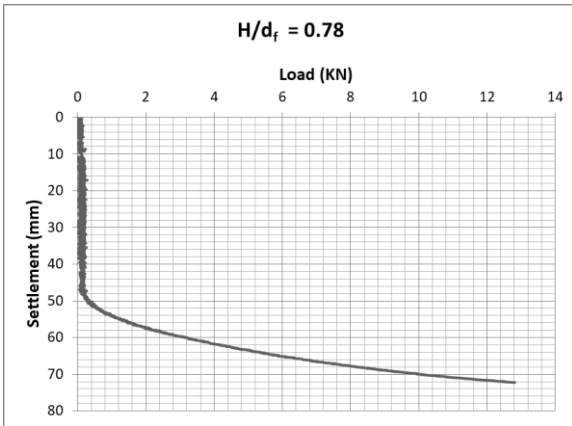


Figure 9. Graph for $H/d_f = 0.78$

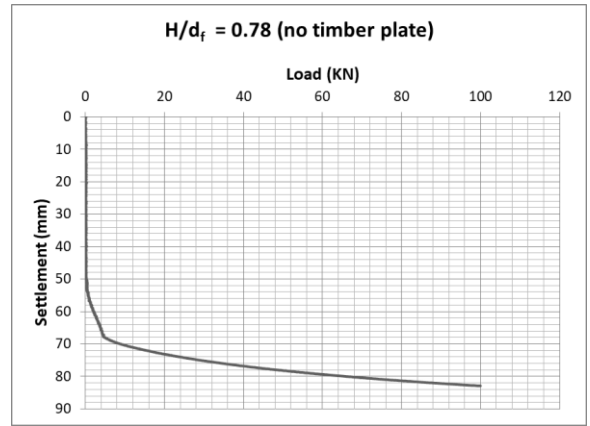


Figure 12. Graph for $H/d_f = 0.78$ (without timber plate)

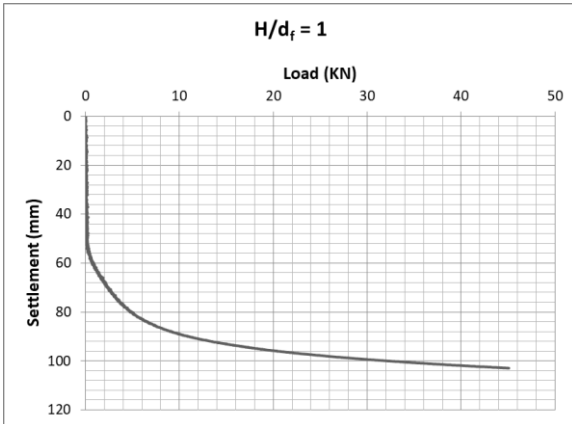


Figure 10. Graph for $H/d_f = 1$

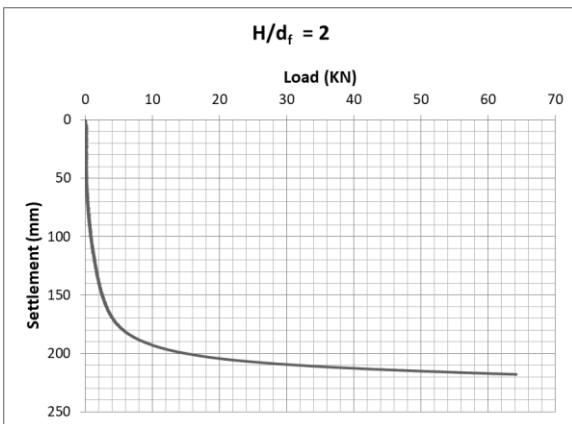


Figure 11. Graph for $H/d_f = 2$

3 DISCUSSION OF THE RESULTS

With regards to the loading tests, the graphs are quite different from those normally plotted in tests with footings. For instance, Figure 13 shows the curves achieved by Cerato and Lutenegger (2006) for the loading tests for a square model footing with dimension of 0.102 m, conducted in sand specimens with a relative density of 87%. In these curves, the ultimate capacity is reached when the loading becomes constant. Comparing with the curves of Figures 9 to 12, there is no tendency towards a constant loading over time for the loading tests with the caisson model. Therefore, the ultimate capacity has not been reached in any of the tests conducted for this paper.

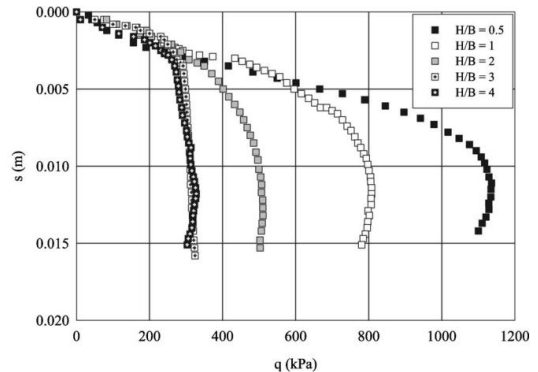


Figure 13 - Loading graphs for a 0.102 m square model footing (Cerato and Lutenegger, 2006)

Also, no significant loading was perceived for a settlement up to 50 mm, which is the height of the skirt of the caisson. Houlby and Byrne (2004) described the following expression to estimate the vertical load for penetration of the skirt without any influence of suction (V):

$$V = \frac{\gamma h^2}{2}(K \tan \delta)(\pi D_o) + \frac{\gamma h^2}{2}(K \tan \delta)(\pi D_i) + \left(\gamma h N_q + \gamma \frac{t}{2} N_\gamma \right) (\pi D t) \quad (3)$$

In the Equation 3, γ is the bulk weight of the soil, h is the settlement of the skirt, D_o and D_i are the external and the internal diameters, respectively, t is the thickness of the skirt and $K(\tan \delta)$ is approximately 0.54. In this equation, the first term of the sum refers to the friction on the internal surface of the skirt, the second term refers to the friction on the external surface of the skirt, and the third term refers to its tip resistance.

Applying, at the Equation 3, $\gamma = 1645 \text{ Kg/m}^3$ (for a dry density of $\gamma_d = 1405 \text{ Kg/m}^3$ and an average moisture content of 17.11%), a vertical load of 0.0658 KN for the penetration of the skirt is obtained. This result indicates the facility of installation of caisson foundations in an offshore field, since there is little resistance between the soil and the skirt. In addition, no tendency towards a constant load over time was observed in all tests.

However, the graphs for the loading tests are quite similar to those of suction installation of caissons. For instance, Figure 14 presents loading tests with caissons performed by Sanham (2003, cited by Houlby and Byrne, 2004), but with suction applied within the footing. Note, for this case, that the part where the loading is zero corresponds to the penetration of the caisson under vertical loads (including self-weight). Moreover, the author applied, for each test, a constant value of suction, whereas, in this project, a constant rate of displacement was used.

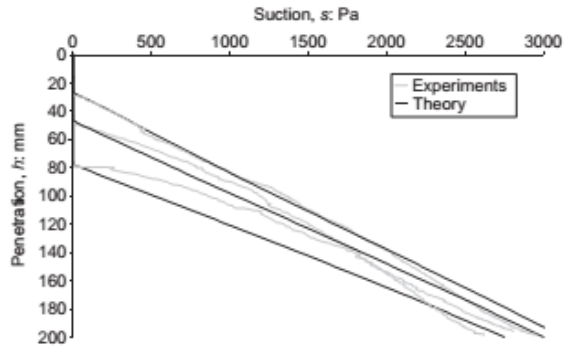


Figure 14 - Laboratory suction-loading tests (Houlby and Byrne, 2004)

Comparing the loading graphs of the four tests, it can be noticed higher loads for smaller sand depths, considering the same settlement value. For instance, Table 5 shows a comparison between the loads for a settlement of 65 mm in each test. Furthermore, comparing the loading tests which $H/d_f = 0.78$, for which the tests were conducted with and without the timber plate, it can be perceived a higher loading for the test with the timber reinforcement compared with the test without the reinforcement. For instance, for a settlement of 65 mm, the loading for the test without reinforcement is 3.846 KN, whereas the loading is 5.919 KN with reinforcement, which represents a difference of 2.073 KN. And this difference increases with the settlement, as represented by Figure 15.

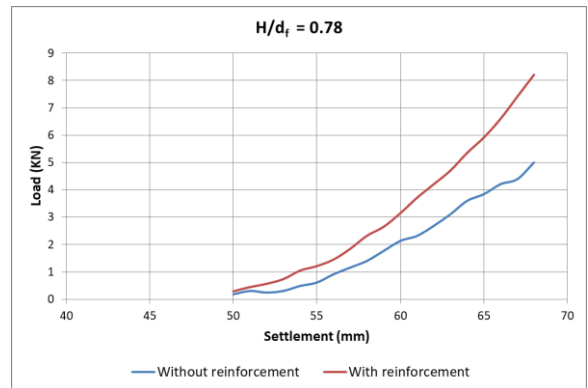


Figure 15 - Loading graphs for $H/d_f = 0.78$

Table 5. Loadings for a settlement of 65 mm

H/ d _f	Loading (KN)
0.78	5.919
1	1.549
2	0.280
0.78 (no timber plate)	3.846

4 CONCLUSIONS

This paper presents the procedures to analyse the capacity of an offshore caisson foundation in sand when there is a hard confining layer underlying the sand layer.

It was difficult to clearly define shear failure of a model foundation in the sand. However, by considering the settlement of the foundation as a failure criteria it was possible to compare the influence of a stiff confining layer (the hard birch plywood plate) on the bearing capacity of the model foundation. The results showed that a stiff confining layer increased the load required to induce 65mm of settlement in the foundation model, relative to no confining layer. This shows that a stiff confining layer at shallow depth positively contributes to the bearing capacity of a shallow foundation in sand. This is in agreement with model foundation tests on loose, medium and dense sand showing that the presence of a hard layer within a certain depth below the foundation can significantly influence the unit load supported by the soil (Cerato & Lutenegeger, 2006).

Finally, some recommendations should be considered for further work, such as:

- Work with different values of sand densities and evaluate their influence;
- Perform tests without the timber plate for other depths of sand, as done for H/d_f = 0.78;
- Adapt the design of the caisson to account the effects of suction in the penetration. In this case, the caisson should be equipped with a valve, allowing the trapped air to scape.

5 ACKNOWLEDGMENTS

This project was developed at the University of Bath, United Kingdom, being part of Science without Borders programme. Then, the authors want to thank the Brazilian agency CNPq, which sponsored the student during the programme, as well as the technicians of the Laboratory of the Architecture and Civil Engineering Department of the University of Bath. Also, the authors want to acknowledge the Engineer Katie Cook, of Arup, who gave an important technical contribution about offshore foundations.

6 REFERENCES

- BS 1377-2:1990. *Methods of test for soils for civil engineering purposes – Part 2: Classification tests*. BSI.
- BS 1377-8:1990. *Methods of test for soils for civil engineering purposes – Part 8: Shear strength tests (effective stress)*. BSI.
- BS EN 636:2003. *Plywood – specifications*. BSI.
- Byrne, B.W., 2011. *Foundation design for offshore wind turbines* [Online]. Oxford: University of Oxford. Available from: http://www.eng.ox.ac.uk/civil/pdf/Geotechnique_Lecture_BWB_2011_Web.pdf, p. 45 [Accessed 7 December 2014]
- Cerato, A.B. and Lutenegeger, P.E, 2006. Bearing capacity of square and circular footings on a finite layer of granular soil underlain by a rigid base. *Journal of Geotechnical and Geoenvironmental Engineering*, 132 (11), pp.1496-1501
- Cotter, O., 2009. *The installation of suction caisson foundations for offshore renewable energy structures*. Thesis (DPhil). University of Oxford, Oxford.
- Houlsby, G.T. and Byrne, B.W., 2004. Design procedures for installation of suction caissons in sand. *Geotechnical Engineering*, 158 (GE3), pp.135-144.